Antibacterial Nanoparticle Monolayers Prepared on Chemically Inert Surfaces by Cooperative Electrostatic Adsorption (CELA)

6 AUTHORS, INCLUDING:

Stoyan K. Smoukov
University of Cambridge
64 PUBLICATIONS   **1,574** CITATIONS

Kyle J M Bishop
Pennsylvania State University
80 PUBLICATIONS   **2,990** CITATIONS

Antibacterial nanoparticle monolayers prepared on chemically inert surfaces by Cooperative Electrostatic Adsorption (CELA)

Sabil Huda, **Stoyan K. Smoukov**, **Hideyuki Nakanishi**, **Bartlomiej Kowalczyk**, **Kyle Bishop**, and **Bartosz A. Grzybowski**[*]
Department of Chemical and Biological Engineering & Department of Chemistry, Northwestern University, 2145 Sheridan Road, Tech. E110, Evanston, IL 60208

Abstract

Cooperative Electrostatic Adsorption (CELA) is used to deposit monolayer coatings of silver nanoparticles on relatively chemically inert polymers, polypropylene and Tygon. Medically relevant components (tubing, vials, syringes) coated by this method exhibit antibacterial properties over weeks to months with the coatings being stable under constant-flow conditions. Antibacterial properties of the coatings are due to a slow release of Ag^+ from the particles. The rate of this release is quantified by the dithiol-precipitation method coupled with Inductively Coupled Plasma Optical Emission Spectrometer (ICP-OES) analysis.

Keywords

Nanoparticles; monolayers; cooperative adsorption; surface modification; silver; antibacterial

Introduction

Silver coatings are well known to confer bacteriostatic and bactericidal properties to surfaces. Although the mechanism of inhibitory action of silver on microorganisms is not fully understood, it is generally believed that it is mediated by the Ag^+ ions which interact with sulfhydryl groups of proteins causing their denaturation and with the bacterial DNA impeding its replication (1–3). Silver coatings are currently used in a variety of medical and consumer products including catheters (4), surgical masks (5), suture threads (6), wound creams and dressings (7), cell phones (Motorola), refrigerators (Whirlpool, Samsung), and recently FDA-approved food packaging (8–9). Traditional solution-based methods for the preparation of such coatings are often material-specific and require numerous coat-rinse steps (10). Various sputtering/evaporation techniques can be effective in coating open, flat surfaces with minimal amounts of silver but they rely on a direct line-of-sight access to the substrate – consequently, these methods give uneven silver coverage on inclined surfaces and cannot be extended to surfaces with overhangs or closed spaces. In this context, silver nanoparticles (AgNPs) present an attractive alternative since they can be deposited from solution onto arbitrarily shaped substrates and can give very thin coatings with total silver content below the safe reference dose (estimated at 5 µg/kg/day -- that is, 25 µg/day for a 5 kg infant and 350 µg/day for a 70 kg adult) (11). However, even with straightforward synthesis and functionalization of the AgNPs (12–13), the general schemes of direct immobilization onto various types of materials

are still lacking. Most work to date has relied on layer-by-layer deposition (10), occlusion of the NPs in a polymer (14), gel (15), or zeolite matrices (16), or on substrate specific chemical interactions (e.g. carbamate-silver interactions in AgNP coated polyurethane foams (17)). We have recently shown that electrostatic forces between charged nanoparticles and substrates presenting residual charges (plasma oxidized PDMS, polyester, polystyrene, glass, etc. (13)) provide a versatile, water-based method for the deposition of high-quality nanoparticle coatings. Formation of the NP coatings is cooperative (18) in the sense that it requires the presence of both negatively and positively charged particles that "seed" the growth of NP monolayers on the substrates being coated (Fig. 1). Here, we demonstrate that this Cooperative Electrostatic Adsorption (CELA) can be extended to materials that are considered relatively chemically inert (19), notably, polypropylene and Tygon-R. Using CELA, we deposit antibacterial AgNP coatings on several medically relevant components/devices such as syringes, tubing, and vials (Fig. 2). The coatings thus formed are stable for prolonged periods of time (weeks to months) in air, under flow of water or in acidic/basic media. In buffer solutions where the component salts screen and weaken the electrostatic interactions between the NPs, the coatings are made stable by crosslinking the deposited particles with dithiols – under such conditions, the "reinforced" films retain their antibacterial properties under constant buffer flow for days to weeks. In all cases, the coatings' antibacterial activity is due to the slow release of Ag^+ from the nanoparticles, whose rate we quantify using a novel dithiol-based precipitation method coupled with Inductively Coupled Plasma Optical Emission Spectrometer (ICP-OES) analysis. The Ag^+ release rate is approximately constant for several months explaining the coatings' long-term antibacterial activity.

Methods

Synthesis of silver nanoparticles

Silver nanoparticles (5.3 ± 1.2 nm) were prepared according to a slightly modified literature procedure (13,20–22). Briefly, 1.72 g of decanoic acid was dissolved in 100 mL of toluene. 32 µL of 98% anhydrous hydrazine was then added, and the solution was left to stir for 30 min. A dilute solution of 25 mg of tetrabutylammonium borohydride (TBAB) in 10 mL of toluene was sonicated for 15 min; 0.1 mL of this solution was then added to the decanoic acid solution. Finally, a solution containing 170 mg of 99% anhydrous silver acetate dissolved in 15 mL of 98% dodecylamine (DDA) solution (1M) in toluene was added to the decanoic acid solution. Upon addition of the final component, the mixture became dark red within ca. 2 min. This solution was left to stir for 1 hr at room temperature and was then left to settle overnight. The sizes of the synthesized NPs were determined using TEM.

Synthesis of gold nanoparticles

Gold nanoparticles (5.5 ± 0.6 nm) were prepared by a modified literature procedure (20–22). Specifically, gold (III) chloride trihydrate $HAuCl_4 \cdot 3H_2O$ (47.2 mg, 0.120 mmol) was dissolved by sonication (~10 min) in 15 mL of toluene solution of DDA (444.2 mg, 2.396 mmol, 20 eq) and DDAB (554.2 mg, 1.198 mmol, 10 eq). In a separate vial, fresh solution of TBAB (117.1 mg, 0.455 mmol, 3.8 eq) and didodecyldimethylammonium bromide, DDAB (221.7 mg, 0.479 mmol, 4 eq) in 6 mL of toluene was prepared and sonicated. TBAB solution was injected to the flask containing gold precursor salt. Color of the solution changed rapidly to dark purple. Reaction was stirred at room temperature overnight, yielding 2–3 nm AuNP seeds. Next, $HAuCl_4 \cdot 3H_2O$ (446.1 mg, 1 mmol) was dissolved by sonication (~10 min) in 115 mL of toluene solution of DDA (5.248 g, 28.306 mmol, 25 eq) and DDAB (2.095 g, 4.529 mmol, 4 eq) followed by the addition of NP seed solution from the previous step. In a separate vial, solution of anhydrous hydrazine (289.9 mg, 9.059 mmol, 8 eq) and DDAB (2.095 g, 4.529 mmol, 4 eq) in 45 mL of toluene was prepared by sonication. Finally, hydrazine solution was added dropwise to the growth solution containing gold salt precursor and NP seeds over the course

of ~30 min. Color gradually became more intense (purple). Reaction was stirred at room temperature overnight yielding gold nanoparticles of average diameter ~ 5.5 nm.

Ligand exchange

A toluene solution of AuDDA or AgDA nanoparticles (~8 µmol/ml, 25 mL, 0.20 mmol) was quenched with 120 mL of methanol to give a black precipitate. The supernatant solution with excess of capping agent and surfactant was decanted, and the precipitate was washed with methanol (50 mL) and re-dissolved in toluene (100 mL) to which a solution of either mercaptoundecanoic acid, MUA, or N,N,N-trimethyl(11-mercaptoundecyl)-ammonium chloride, TMA, thiol (100 µmol) in 10 mL of CH_2Cl_2 was added while stirring. The precipitate of thiol-coated metal NPs was allowed to settle down, the mother-liquid solution was decanted, and the solid was washed with CH_2Cl_2 (3×50 mL). The precipitate was then dissolved in 5 mL of methanol upon sonication. The MUA NPs were deprotonated with 25% methanolic solution of $N(CH_3)_4OH$ (0.1 mL, 0.25 mmol), precipitated with acetone (30 mL), and washed with acetone (2×30 mL). The TMA NPs were precipitated with ethyl acetate (100 mL) and washed with CH_2Cl_2 and acetone. Finally, all the precipitates of thiol coated NPs were dried and dissolved in deionized water to obtain ~10 mM (in terms of metal atoms) solutions of NPs.

Growth of bacterial cultures and coating testing

Mueller-Hinton Agar plates (Hardy Diagnostics), *E. coli* (ATCC 25922), and *S. aureus* (ATCC 25923) (PML Microbiologics), as well as bacterial growth media LB-Miller and Trypticase Soy broth were obtained from VWR. Bacteria were streaked on LB-agar plates and grown at 37 °C for 16 hrs when colonies were isolated. Sterile batches of LB-broth were inoculated with the colonies, and grown overnight (16 hrs). Bacterial concentrations were quantitated using a Neubauer cytometer and subsequently using the serial dilution method and showed that they had density of $2.08×10^9$ cfu/mL for *E. coli* and $1.98×10^9$ for *S. Aureus*. The Kirby-Bauer disk diffusion test (10), was used to test coatings for antibacterial activity. After Mueller-Hinton (MH) agar plates were inoculated with bacteria and left to stay for ~2–3 min to dry, uncoated (control) and NP-coated disks were placed onto the gel. The plates were turned upside down and incubated at 37 °C for 16 hrs.

Flow experiments

1× PBS buffer (Cellgro, cat. #21-040-CV) was obtained from VWR and was used as received. Polypropylene 3 mL syringes coated with a mixture of MUA-coated and TMA-coated NPs were immersed in a solution of 10 mM 1,6-hexanedithiol (VWR) in acetone for 12 hrs. After the dithiols crosslinked the NPs, the syringes were connected to a peristaltic pump which drove the flow of PBS at the rate of 1–1.3 mL/min for several days up to two weeks.

Measurement of the rate of Ag⁺ release from AgNPs

6 mL of 113 mM freshly prepared AgMUA (or AgTMA) NP solution was allowed to "age" for periods between one and 120 days. During this time, small (50 µL) aliquots were taken from the solution, diluted to 0.5 mL with acetone and precipitated by addition of 0.1 mL of 97% 1,6-hexanedithiol (VWR). The nanoparticle-free supernatant was then analyzed for the content of Ag^+ ions using Inductively Coupled Plasma (Varian Vista MPX ICP-OES) measurements.

Results and Discussion

Coatings were deposited from 0.5 – 2 mM (in terms of atoms of each metal) solutions containing equal amounts of like-sized (~5 nm, see Methods) but oppositely charged silver nanoparticles (AgNPs) stabilized with self-assembled monolayers (SAMs) of ω-functionalized alkane thiols

(24). Half of the NPs in solution were coated with the positively charged *N,N,N*-trimethyl(11-mercaptoundecyl)-ammonium chloride (TMA, ProChimia Poland) and half with the negatively charged mercaptoundecanoic acid (MUA, deprotonated at pH = 11; ProChimia) (13,20–21, 25). Despite the presence of both positively and negatively charged NPs, the solutions were stable for weeks to months (for further experimental details, see (13,21,26)).

The substrates used in this study were, polypropylene pipette tips and vials (from Fisher Scientific), polypropylene syringes (from BD), and PVC-based Tygon R 3603 tubing (27) (from St. Gobain Corp.). Immediately prior to NP deposition, all materials/components were washed with water, dried under nitrogen stream, and exposed to oxygen plasma (SPI, Plasma Prep II) for 1–2 min. The oxygen plasma treatment introduced hydrophilic, ionizable groups onto the surface of the materials (28). For polypropylene and Tygon/PVC, the relevant groups were (29) hydroxyl and carboxyl; when oxidized, these polymers had the values of φ_{surf} around ca. - 0.05 V. The oxidized substrates exhibited reduced bacterial adhesion but not the antibacterial activity – this observation agrees with previous studies (28).

To deposit NP coatings, the oxidized substrates were immersed in the coating solution for ~ 10–15 min. Subsequently, they were rinsed for 20–30 sec. in a large beaker of deionized water, and were dried in a stream of dry air. The morphology of the coatings was analyzed by SEM (Fig. 1 and Fig. S1) which evidenced formation of nanoparticle monolayers with surface coverages ca. $70 \pm 8\%$ (standard deviation based on the analysis of five SEM samples, ca. 1000 NPs in total). The coatings form as a result of cooperative electrostatic interactions (13) between the charged nanoparticles and between the nanoparticles and the oxidized substrate whose surface bears residual negative charge developed during plasma oxidation (Fig. 1). Importantly, coatings form neither from pure MUA NPs (because of repulsions between particles and the substrate, Fig. 1a) nor pure TMA NPs (because of repulsions between adsorbed particles, Fig. 1b) and are deposited only from mixtures of oppositely charged NPs (Fig. 1c). With such mixtures, the energetically unfavorable adsorption of negatively charged MUA AgNPs onto the negatively charged substrate is compensated by the favorable $^+/-$ interactions in the adsorbed "patchy" coatings and also by the screening of electrostatic repulsions between like-charged particles by the NPs metal cores (so that electrostatic forces are short-ranged). The adsorption process self-terminates when a charge-balanced monolayer $(\sum Q_{NP(+)} + \sum Q_{NP(-)} = 0)$ is deposited so that there is no net charge to drive further adsorption (13).

Optically, the coatings had characteristic hues (Fig. 1d and Fig. 2) due to the surface on plasmon resonance (SPR) of the constituent nanoparticles (22). For example, all-silver AgMUA/AgTMA coatings had a maximum of adsorption at λ_{max} ~ 430 nm and appeared orange-red; coatings incorporating gold particles (e.g., AuMUA/AgTMA) had additional adsorption maximum at λ_{max} ~ 550 nm and appeared dark pink to violet. These colors were vivid owing to the extremely high extinction coefficients of the NPs (e.g., ε ~ 6,000 $M^{-1}cm^{-1}$).

Antibacterial properties of the coatings were studied by the Kirby-Bauer diffusion test (10) using either freshly prepared coatings or coatings that were kept under air or under $1\times$ Phosphate buffer solution flow (PBS) (i.e., under conditions relevant to the storage and use of the medical components in Fig. 2) for periods up to several weeks. A small piece of the coated material was placed onto a thin agar gel inoculated with either Gram-negative *E. coli* or Gram-positive *S. Aureus* bacteria (see Methods). Despite low content of silver, ~2.3 µg/cm², the AgMUA/AgTMA coatings deposited on all tested substrates had excellent and long-lasting antibacterial properties. Figures 3a and 3b show typical zones of inhibition (ZoI's) – that is, regions over which the bacterial growth is absent – around coated PVC substrates. Similar ZoI's were observed around other NP-coated materials but not around the uncoated "controls". Also, the antibacterial activity derived from the presence of AgNPs, since coating incorporating

other types of NPs gave smaller zones of inhibition (cf. Fig. 3c,d for the AuMUA/AgTMA vs. AgMUA/AgTMA comparison).

Once formed, the coatings subject to air or kept under the constant flow of water, dilute-acid (< ~20 mM) or base (< ~20 mM) retained antibacterial activity for at least several months and at flow rates 1–5 mL/min. SEM imaging indicates that during this time the constituent NPs were structurally stable and that there was no degradation or coalescence of the constituent particles. In the case of coated syringes (Fig. 2d), the coatings retained their structural integrity and antimicrobial activity when the piston was moved back and forth multiple times (>20) in either wet or dry state. However, under the flow of buffers (e.g., PBS), the coatings disintegrated within ca. 1 day. The reason for this is that the salts in the buffer screen the attractive electrostatic interactions between the neighboring NPs and between the NPs and the residual charges on the substrate. Since stability of the coatings under buffer flow is one of the important criteria for their potential use in medical devices, we sought a method to "reinforce" the coatings. A straightforward solution to the problem was to crosslink the deposited NPs with dithiols bridging the nearby particles (Fig. 4a). In a typical procedure, this was achieved by soaking the as-prepared coatings in a 10 mM solution of 1,6-hexanedithiol in acetone overnight. Once the crosslinking was complete, the individual NPs could not dissociate from the substrate and the "reinforced" coatings remained stable and antibacterial after being kept under continuous flow of a buffer solution for days to weeks (Fig. 4b)

Given the morphological stability of the coatings, an important question arises how these "apparently unchanging" coatings can confer bacteriostatic activity. As mentioned in the introductory paragraph, bacteriostatic effects of silver are commonly attributed to Ag^+ cations. The AgNPs comprising our coatings, however, are composed of metallic silver, Ag^0 nanoparticle cores passivated/stabilized by the self-assembled monolayers (SAMs) of TMA or MUA alkane thiols. To reconcile these two observations, there should exist a mechanism, by which silver atoms comprising the NP cores are oxidized and released from these nanoparticles. Although the SAMs we used bind to silver tightly ($\Delta G_{adsorption}$ ~ - 5.5 kcal/mol (30)), it is known that these monolayers are marginally permeable to oxygen which can oxidize metallic silver to Ag^+ ($2RSH + \frac{1}{2}O_2 \rightarrow RSSR + H_2O$) (31). If this is so, the concentration of Ag^+ present in solution containing AgNPs should increase with time. Furthermore, since the structure of the NPs comprising the coatings does not change perceptibly over the course of weeks to months (as verified by SEM measurements; cf. above), we expect this release to be slow and the amounts of released silver low.

We verified these hypotheses by a combination of dithiol NP precipitation and Inductively Coupled Plasma Optical Emission Spectrometer (ICP-OES), which is a highly sensitive method of metal detection. In the experiments, we used ~100 mM AgNP solutions rather than monolayer coatings, since the release from the latter was below the detection limit of the ICP-OES spectrometer used (~0.1 ppm). To make detection specific to free Ag^+ cations (and not Ag^0 in the NPs), we developed a selective precipitation procedure in which a large excess (~ 10^7 molecules per one NP) of alkane dithiols, $HS-(CH_2)_6-SH$ was added to the solution prior to ICP-OES analysis. As we have shown earlier (32), dithiols crosslink silver NPs in solution, causing them to aggregate and precipitate. Importantly, in doing so, they do not precipitate Ag^+ cations, which remain is solution (33) (Fig. 5a).

In this way, the amount of Ag^+ can be quantified. This is illustrated in Figure 5b which shows the dependence of Ag^+ release as a function of time. The fraction of silver atoms that are oxidized and released from the NPs, $\chi = [Ag^+]/([Ag^0]+ [Ag^+])$, increases with time approximately linearly and reaches ~3% after $t = 120$ days. Interestingly, the observed rate of release can rationalize the dimensions of the zones of inhibition observed in the Kirby-Bauer test (see Fig. 3). This can be shown by using the well known formula that relates the thickness

of the inhibition zone (10, 34–35), H_{ZoI}, around a circular source of an antibacterial agent to this agent's concentration, c, and diffusion coefficient, D ($\sim 10^{-5}$ cm^2/sec for Ag$^+$ in wet hydrogels (36)), $H_{Zol} = \sqrt{\ln(c/c^*)Dt}$. In this expression, c^* is the minimum amount of the agent (here, Ag$^+$) required to stop bacterial growth completely. In independent experiments using AgCl salt, we determined this concentration to be $c^* \sim 2.5 \times 10^{-5}$ µmol/mL, which is close to the value reported by others (37). Using this value and estimating the concentrations of Ag$^+$ ions (released from NP-coated disks into 1-mm-thick agar gel layer) from Figure 4b gives the thicknesses of ZoI commensurate with those observed experimentally. For instance, for $t = 16$ hrs, the estimated concentration of released [Ag$^+$] $\sim 2.6 \times 10^{-5}$ µmole/mL yields $H_{ZOI} \sim 1.5$ mm, close to the H_{ZOI} observed experimentally for both *E.coli* (1.4 ± 0.3 mm on all materials) and *S.aureus* (1.9 ± 0.4 mm, again, for all types of substrates; standard deviations are based on ten plating experiments involving both dithiol-reinforced and non-reinforced coatings).

Conclusions

In sum, these findings indicate that the NPs in the monolayers act as controlled-release elements conferring antibacterial activity to the coated surfaces. The ability to use cooperative electrostatic adsorption in conjunction with medically relevant and otherwise hard to coat materials suggests applications of this method for long-term antibacterial protection of medical components/devices. In this context, the characteristic hues of the coatings provide easily discernible indication of their presence and structural integrity. In the future, this method could be extended to AgNPs coated with different types of SAMs to regulate the speed of Ag$^+$ release and to particles of different metal cores (e.g., antifungal copper NPs).

Supplementary Material

Refer to Web version on PubMed Central for supplementary material.

Acknowledgments

References

1. Son WK, Youk JH, Lee TS, Park WH. Macromol. Rapid Commun 2004;25:1632–1637.

2. Feng QL, Wu J, Chen GQ, Cui FZ, Kim TN, Kim JO. J. Biomed. Mater. Res 2000;52:662–668. [PubMed: 11033548]

3. Clement JL, Jarrett PS. Met. Based Drugs 1994;1:467–482. [PubMed: 18476264]

4. Pai MP, Pendland SL. Ann. Pharmacother 2003;37:192–196. [PubMed: 12549945]

5. Li Y, Leung P, Yao L, Song QW, Newton E. J. Hosp. Infect 2006;62:58–63. [PubMed: 16099072]

6. Blaker JJ, Nazhat SN, Boccaccini AR. Biomaterials 2004;25:1319–1329. [PubMed: 14643606]

7. Tredget EE, Shankowsky HA, Groeneveld A, Burrell R. J. Burn Care Rehabil 1998;19:531–537. [PubMed: 9848045]

8. Del Nobile MA, Conte A, Cannarsi M, Sinigaglia M. J. Food Saf 2009;29:14–25.

9. Quintavalla S, Vicini L. Meat Sci 2002;62:373–380.

10. Lee D, Cohen RE, Rubner MF. Langmuir 2005;21:9651–9659. [PubMed: 16207049]

11. Fung MC, Bowen DL. J. Toxicol.-Clin. Toxicol 1996;34:119–126. [PubMed: 8632503]

12. Nikhil RJ, Peng X. J. Am. Chem. Soc 2003;125:14280–14281. [PubMed: 14624568]

13. Smoukov SK, Bishop KJM, Kowalczyk B, Kalsin AM, Grzybowski BA. J. Am. Chem. Soc 2007;129:15623–15630. [PubMed: 18041837]

14. Cioffi N, Torsi L, Ditaranto N, Tantillo G, Ghibelli L, Sabbatini L, Bleve-Zacheo T, D'Alessio M, Zambonin PG, Traversa E. Chem. Mat 2005;17:5255–5262.

15. Lee WF, Huang YC. J. Appl. Polym. Sci 2007;106:1992–1999.

16. Kawahara K, Tsuruda K, Morishita M, Uchida M. Dental Materials 2000;16:452–455. [PubMed: 10967196]

17. Prashant J, Pradeep T. Biotech. Bioeng 2005;90:59–63.

18. Tretiakov KV, Bishop KJM, Kowalczyk B, Jaiswal A, Poggi MA, Grzybowski BA. J. Phys. Chem. A 2009;113:3799–3803. [PubMed: 19228008]

19. http://www.vp-scientific.com/Chemical_Resistance_Chart.htm

20. Kalsin AM, Fialkowski M, Paszewski M, Smoukov SK, Bishop KJM, Grzybowski BA. Science 2006;312:420–424. [PubMed: 16497885]

21. Kalsin AM, Kowalczyk B, Smoukov SK, Klajn R, Grzybowski BA. J. Am. Chem. Soc 2006;128:15046–15047. [PubMed: 17117829]

22. Kalsin AM, Pinchuk AO, Smoukov SK, Paszewski M, Schatz GC, Grzybowski BA. Nano Lett 2006;6:1896–1903. [PubMed: 16967998]

23. Kalsin AM, Kowalczyk B, Wesson P, Paszewski M, Grzybowski BA. J. Am. Chem. Soc 2007;129:6664–6665. [PubMed: 17488007]

24. Witt D, Klajn R, Barski P, Grzybowski BA. Curr. Org. Chem 2004;8:1763–1797.

25. Measurements performed on a Zeta-Sizer instrument for individual NP solutions (i.e.`, before mixing) showed that the typical values of the surface potentials at pH = 10–11 were +30–50 mV for TMA NPs and −40–60 mV for MUA NPs.

26. Bishop KJM, Grzybowski BA. Chem. Phys. Chem 2007;8:2171–2176. [PubMed: 17763505]

27. Material properties and specifications for Tygon R 3603 can be found at: http://www.tygon.com/Data/Element/Node/ProductLine/Product_line_edit.asp? ele_ch_id=L0000000000000001495

28. Balazs DJ, Triandafillu K, Chevolot Y, Aronsson BO, Harms H, Descouts P, Mathieu HJ. Surf. Interface Anal 2003;35:301–309.

29. O'Kell S, Henshaw T, Farrow G, Aindow M, Jones C. Surf. Interf. Anal 1995;23:319–327.

30. Karpovich DS, Blanchard GJ. Langmuir 1994;10:3315–3322.

31. Bagiyan GA, Koroleva IK, Soroka NV, Ufimtsev AV. Russ. Chem. Bull 2003;52:1129–1134.

32. Klajn R, Bishop KJM, Fialkowski M, Paszewski M, Campbell CJ, Gray TP, Grzybowski BA. Science 2007;316:261–264. [PubMed: 17431176]

33. The dithiols did not cause perceptible precipitation of Ag^+. To verify this, we performed a set of experiments in which 0.1 mL of dithiol was added to 10 mL solutions of $AgNO_3$ (either 0.1 mM or 1 mM in deionized water). The solutions were then centrifuged at 2000g for 20 min and the supernatant was analyzed using ICP-OES. In all seven samples measured, the content of silver ions was > 97% of the original one indicating that only negligible fraction (if any) of the silver cations is removed/precipitated by the disulfides.

34. Kavanagh, F. Analytical Microbiology. Academic Press Inc.; 1963.

35. Cooper KE. Nature 1955;176:510–511. [PubMed: 13253602]

36. Bensemann IT, Fialkowski M, Grzybowski BA. J. Phys. Chem. B 2005;109:2774–2778. [PubMed: 16851286]

37. Morones JR, Elechiguerra JL, Camacho A, Holt K, Kouri JB, Ramirez JT, Yacaman MJ. Nanotechnology 2005;16:2346–2353.
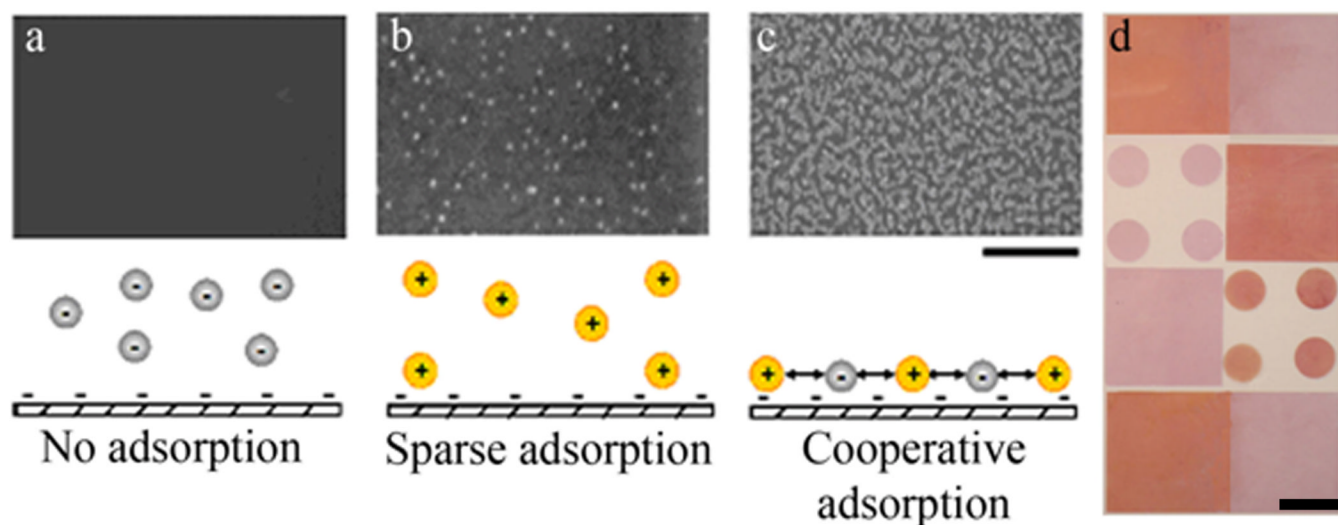
FIGURE 1.
Cooperative electrostatic adsorption. **(a)** Negatively charged NPs do not adsorb onto oxidized surfaces presenting residual negative charge. **(b)** Similarly, positively charged NPs give only very sparse coatings (~5% surface coverage) due to the repulsions between adsorbed particles. **(c)** Mixtures of positively and negatively charged nanoparticles adsorb cooperatively and yield dense coatings (~70% surface coverage). Scale bar for (a)–(c) is 200 nm; in all cases, the NPs are deposited on silicon. **(d)** Coatings deposited on glass and composed of only silver NPs (e.g., AgMUA and AgTMA) appear orange-red; those comprising gold and silver particles (e.g., AuMUA and AgTMA) are violet. Scale bar in (d) represents 10 mm. Also see fig. S1 in the Supporting Information.
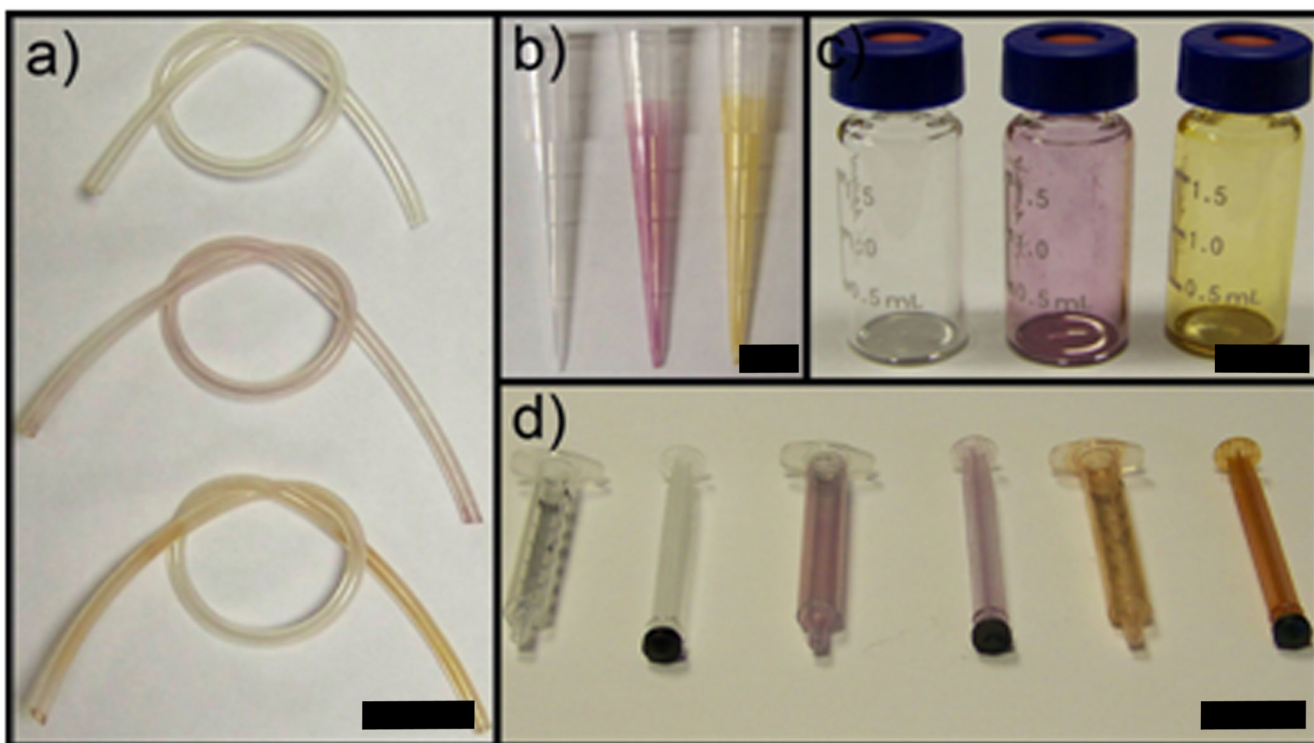
FIGURE 2.
Examples of medically relevant components coated with bacteriostatic NP monolayers of oppositely charged nanoparticles. **(a)** Tygon-R tubing (scale bar = 16 mm) **(b)** Polypropylene micro-pipette tips (scale bar = 8 mm) **(c)** Glass vials (scale bar = 8 mm) (d) Polypropylene syringes (scale bar = 32 mm). Yellow-orange coatings are made of AgMUA/AgTMA; pink coatings, from AuMUA/AgTMA. Uncolored pieces are shown for reference. All coatings were deposited by immersion (~10 min) in aqueous NP solutions.
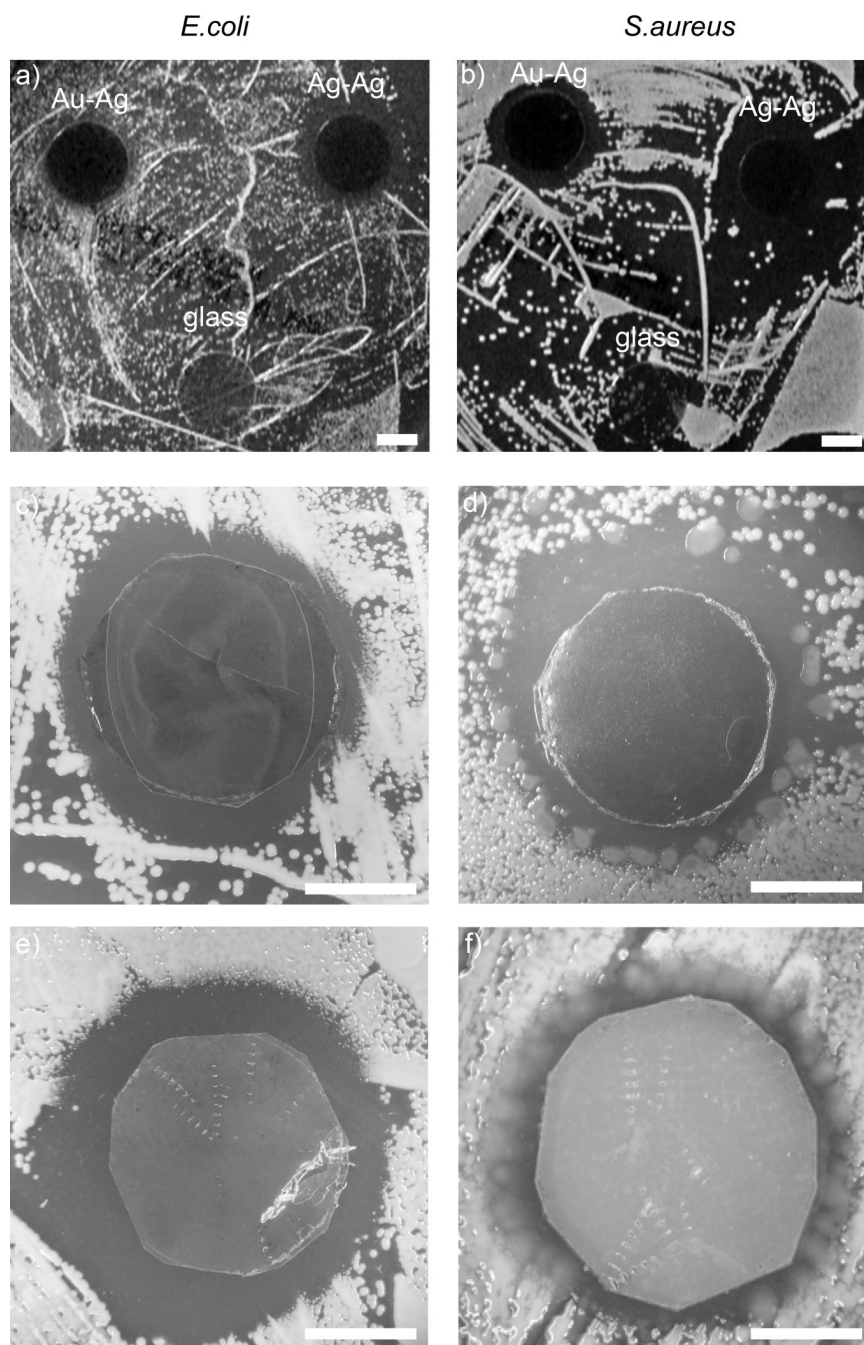
E.coli   *S.aureus*

FIGURE 3.
(a,b) Comparison of antibacterial properties of all-silver, AgMUA/AgTMA, and gold-silver, AuMUA/AuTMA, coatings deposited on polypropylene disks (all disk are 10 mm in diameter and are delineated by dashed lines). For both types of bacteria, *E.Coli* (left column) and *S.Aureus* (right column), the bacteria-free (clear) zones of inhibition are more pronounced for the all-silver coatings than for silver-gold coatings. Note the absence of inhibition around uncoated glass disks. **(c,d)** Zones of inhibition around pieces of PVC-based Tygon-R coated with AgMUA/AgTMA and tested on *E.Coli* (c) and on *S.Aureus* (d). **(e, f)** Zones of inhibition for Nylon coated with AgMUA/AgTMA tested on (e) *E.coli* and (f) *S.Aureus*. All scale bars (a–f) correspond to 5 mm. All images were taken 16 hrs after plating the bacteria.
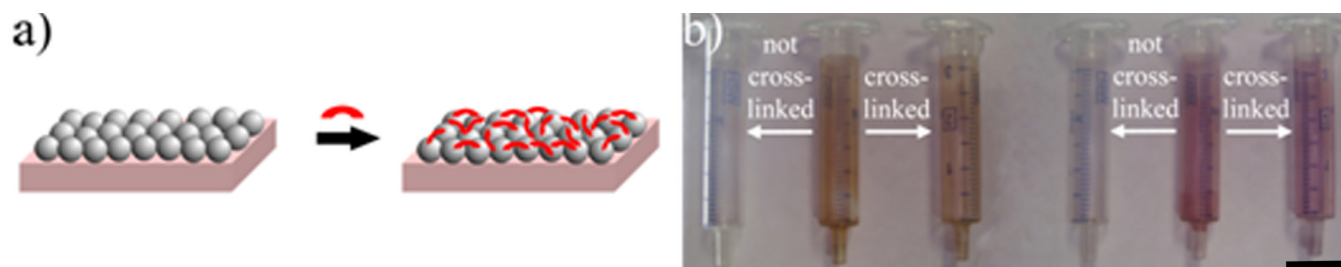
FIGURE 4.
(a) Scheme illustrating crosslinking of the deposited NP coatings with alkane dithiols (red arcs). **(b)** The middle images in each triad show as-prepared coatings (all-Ag on the left; mixed Ag/Au on the right) deposited on the inner surface of polypropylene syringes. Under flow of buffer (here, PBS, 1.3 mL/min), the coatings disintegrate overnight and the syringes loose the characteristic hue. When, however, the coatings are reinforced by crosslinking, the coatings remain stable under buffer flow for days to at least two weeks. Stability was confirmed by the lack of changes in the coating's UV-Vis spectra. The scale bar corresponds to 17 mm.
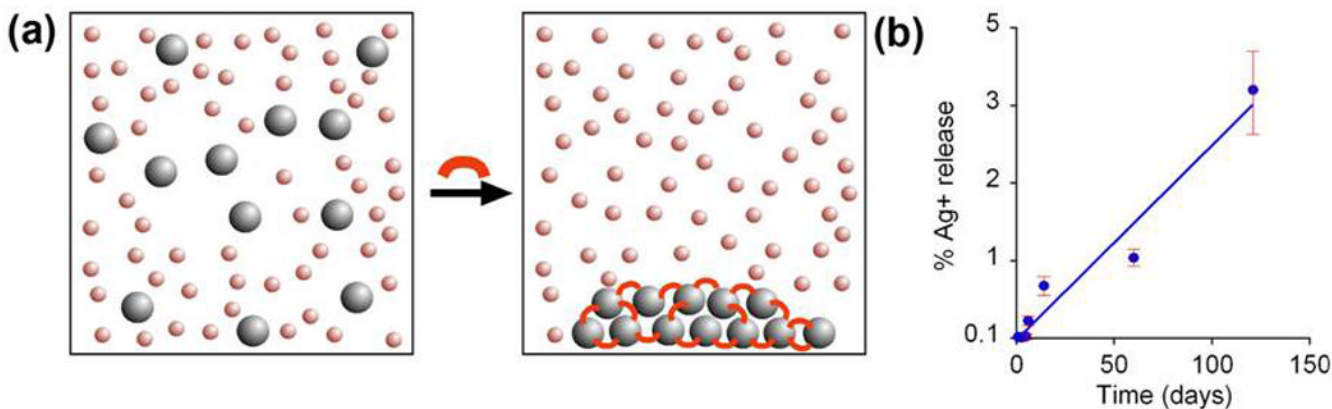
FIGURE 5.
(a) Scheme of the selective precipitation method in which addition of dithiols (red arcs = HS-$(CH_2)_6$-SH) causes crosslinking and aggregation of AgNPs (larger, gray circles) but not of Ag^+ ions (smaller, brown circles). The concentration of ions released from the NPs and remaining in solution can be then determined by ICPOES. **(b)** Percentage of Ag^+ cations released from AgNPs as a function of time. Error bars are based on the measurements of six samples for each time point. Measurements for each nanoparticles "leak" the cations at an approximately constant rate. Note that after four months, only ~3% of NP contents leaks out indicating that the NP coatings can provide long-term antibacterial protection.